Available online at www.sciencedirect.com
ScienceDirect
Ceramics International 38S (2012) S287–S290
CERAMICS INTERNATIONAL
www.elsevier.com/locate/ceramint

Influence of Mn^{2+} on the electrical properties of textured KNN thick films

Fang Fu [a], Bo Shen [a], Jiwei Zhai [a,*], Zhengkui Xu [b], Xi Yao [a]

[a] Functional Materials Research Laboratory, Tongji University, Shanghai 200092, China
[b] Department of Physics and Materials Science, City University of Hong Kong, Hong Kong

Available online 4 May 2011

Abstract

Textured $K_{0.5}Na_{0.5}NbO_3$ thick film was prepared by the reactive templated grain growth method. The effects of Mn^{2+} doping on the phase structure, microstructure and electrical properties of the $K_{0.5}Na_{0.5}NbO_3$ textured thick film were investigated. The grain orientation degree decreased with increasing Mn^{2+} and reduced to 50% for the thick film with 5 mol% Mn^{2+}. The addition of Mn^{2+} improved the microstructure of the thick film. The electric properties of the thick film were also enhanced because of the high densification, the vacancy compensation effect and the acceptor doping effects of Mn^{2+}. The $K_{0.5}Na_{0.5}NbO_3$ thick film with 2 mol% Mn^{2+} doping possessed the optimum properties: $P_r = 3.05\ \mu C/cm^2$, $E_c = 4.79$ kV/cm, $J = 4.6 \times 10^{-6} A/cm^2$ (at 25 kV/cm) and $d_{33}^* = 124$ pm/V.

Keywords: A. Films; A. Tape casting; C. Electrical properties; D. Perovskites

1. Introduction

The miniaturization of electroceramics has shown an increasing trend for the development of microelectromechanical systems (MEMS) such as microsensors and microactuators [1,2]. The thick film technology is appreciated for integration, not only for its low dimension, but also for the rapid reduction on the driving voltage. Meanwhile, the evident deteriorate electric properties of the thin films can be avoided for the thick films. Lead zirconate titanate (PZT) is the most popular materials for thick film [3]. However, lead free piezoelectric materials have been desired from the viewpoint of environmental protection over the last few years, especially after the announcement of draft directives on waste from electrical and electronic equipment (WEEE) and restriction of hazardous substances (RoHS) [4].

The $K_{0.5}Na_{0.5}NbO_3$-based (KNN) compositions have shown great advantages over other typical lead free piezoelectric material system [5]. However, the piezoelectric properties of the KNN materials are still inferior to PZT based ones. In recent years, the composition modification is widely used to improve the performance of the KNN ceramics, besides, the grain oriented technology is also considered to be one of the effective approaches to improve the piezoelectric properties of the ceramics [6,7]. Whereas, the high loss tangent comes to be a significant problem for the KNN textured thick film. The addition of manganese acceptor has been verified to be an effect way to reduce the loss tangent of the KNN ceramics [8,9]. Furthermore, the volatilization of alkali metal ions in the thick film supposed to be more seriously than in bulk ceramics. The addition of Mn^{2+} compensates the charge defects generated from the volatilization of alkali metal ions to improve the properties of the thick film.

In our present work, the Mn ions were added to decrease the loss tangent of the KNN textured thick film. The influence of the Mn^{2+} dopant on the phase structure, microstructure and electric properties of the KNN textured thick film was investigated.

2. Experimental

The KNN powders were prepared with sodium carbonate (Na_2CO_3, 99.8%, Sinopharm Chemical Reagent Co. Ltd), potassium carbonate (K_2CO_3, 99.0%, Sinopharm Chemical Reagent Co. Ltd) and niobium oxide (Nb_2O_5, 99.5%, Sinopharm Chemical Reagent Co. Ltd) as raw materials via the conventional solid state reaction. The KNN–*x*Mn matrix was prepared with the pre-calcined KNN powders and *x* mol%

* Corresponding author. Tel.: +86 21 65980544; fax: +86 21 65985179.
E-mail address: apzhai@tongji.edu.cn (J. Zhai).

0272-8842/$36.00
doi:10.1016/j.ceramint.2011.04.103

($x = 0$, 1, 2 and 5) manganese carbonate (Mn_2CO_3, Mn 44%, Alfa Aesar, A Johnson Matthey Company). The $NaNbO_3$ (NN) plate-like particles with the sharp of a thickness about 0.5 μm and a width ranged from 10 μm to 20 μm were fabricated by the double molten salt method with $Bi_{2.5}Na_{3.5}Nb_5O_{18}$ as precursor. The mixture of 90 wt% matrix and 10 wt% plate-like NN particles was added in the solution composed with toluene and dehydrated alcohol and then this suspension was milled for 15 h. The binder (LS model, produced by Lingguang Electric Chemical Materials Technology Corporation, Zhaoqing City, China) was added to the suspension and milled for anther 3 h to stabilize the casting slurry. This slurry was tape cast with conventional tape-casting equipment. The green thick film was cut and pressed on the alumina substrate with Ag–Pd bottom electrode by isostatic pressing under 200 MPa. The green film was annealed at 550 °C to remove the organic substance and then sintered at 1150 °C for 2 h.

Phase structures of the thick films were investigated with X-ray diffraction (XRD, D8 Advanced, Bruker AXS, Germany) with Cu Kα radiation. The degree of the grain orientation can be represented by the Lotgering's factor F [10].

The microstructures of the specimens were examined by scanning electron microscopy (SEM, JSM EMP-800, Japan). In order to determine the electric properties of the specimens, the gold electrode with a thickness of 80 nm and a diameter of 0.5 mm sputtered on the surfaces of the thick films. Frequency dependences of the dielectric constant and loss were measured from 10 kHz to 2 MHz by using a high-precision LCR meter (HP 4284A, Aglient, USA). Leakage current density J was tested with electrometer (Keithley 6517A, Cleveland OH, USA). The P–E hysteresis loops and the longitudinal displacement field curves were measured by the ferroelectric test systems (Precision Premier II, USA) connected with a Miniature Plane-mirror Interferometer and the accessory Laser Interferometric Vibrometer (SP-S 120/500 Model, German).

3. Results and discussion

Fig. 1 shows the XRD patterns of the Mn^{2+} doped KNN textured thick films. All thick films possess perovskite structures. Some impurity phases identified as $K_2Nb_8O_{21}$ and Nb_2O_5 are observed. The peak intensity of impurity phase increases with increasing Mn^{2+} concentration. The appearance of impurity phase properly dues to the volatilization of the alkali metal ions at 1150 °C. The detailed XRD patterns performed in the 2θ range of 39.5°–40.5° and 45.5°–47° are shown in Fig. 1(b) and (c), respectively. The single peak near 40° and 46° indicates the pseudocubic structure of the textured KNN thick film. The structures of the samples added with Mn^{2+} have the features of tetragonal symmetry evidenced by the splitting of (0 0 2)/(2 0 0) peaks at 2θ around 46°. This indicates that the crystal structure of the KNN thick film transformed from a pseudocubic into tetragonal phase with the addition of the Mn^{2+}. The F values calculated from the XRD patterns of the thick films also illustrate in Fig. 1(a). The F value gradually decreased from 63 to 50% with the addition of Mn^{2+}.

Fig. 2 shows the SEM micrographs of the textured KNN thick films with $x = 0$, 0.01, 0.02 and 0.05. The thick film without Mn^{2+} doping has a very loose structure and a large amount of the pores owing to the residual organic vehicle and the volatilization of the alkali metal ions. The distribution of the porosity decreases after a small amount of Mn^{2+} adding. The doping Mn^{2+} leads to the distortion of crystalline lattice and then promotes the sintering process. However, an abnormal large grain marked with A in Fig. 2(d) is observed in the thick film with $x = 0.05$. The abnormal grain growth usually occurred in the presence of the liquid phase, so the addition of Mn^{2+} in the thick film seems to lead to the liquid phase. Whereas, the presence of the liquid phase needs more detailed analysis which does not conducted in our present study.

Fig. 3 illustrates the polarization hysteresis loops of the Mn^{2+} doped KNN textured thick films. The polarization hysteresis loop of the KNN textured thick film shows a low remnant polarization (P_r) of 0.77 μC/cm^2. This may caused by the structure defects such as porosity and charge defects induced by the volatilization of the alkali metal ions. These defects deplete part of the electric field and reduce the effective electric field applied on the thick film. The P_r was found to increase with the addition of Mn^{2+} as shown in the inset of Fig. 3 and reached to its maximum value of 6.82 μC/cm^2 for the thick film with $x = 0.05$. The coercive electric field (E_c) decreased with increasing Mn^{2+} concentration and reaches to a minimum value of 4.79 kV/cm for the thick film with $x = 0.02$. These should be attributed to the improved microstructure and the compensation effect on the charge defects by the addition of Mn^{2+}.

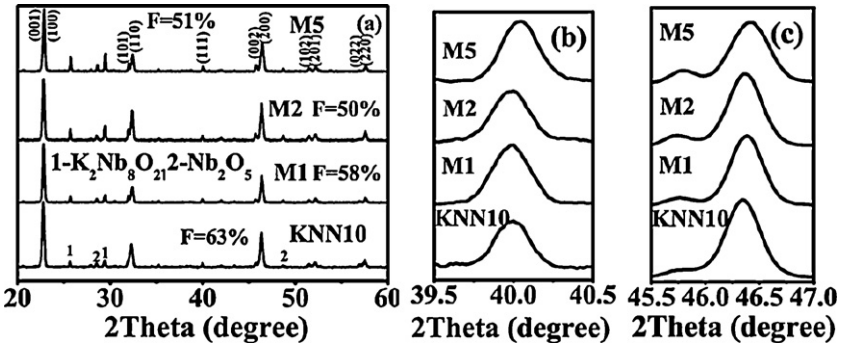

Fig. 1. XRD patterns of KNN–xMn ($x = 0$, 0.01, 0.02 and 0.05) thick films in the 2θ range of (a) 20°–60°; (b) 39.5°–40.5°; and (c) 45.5°–47°.

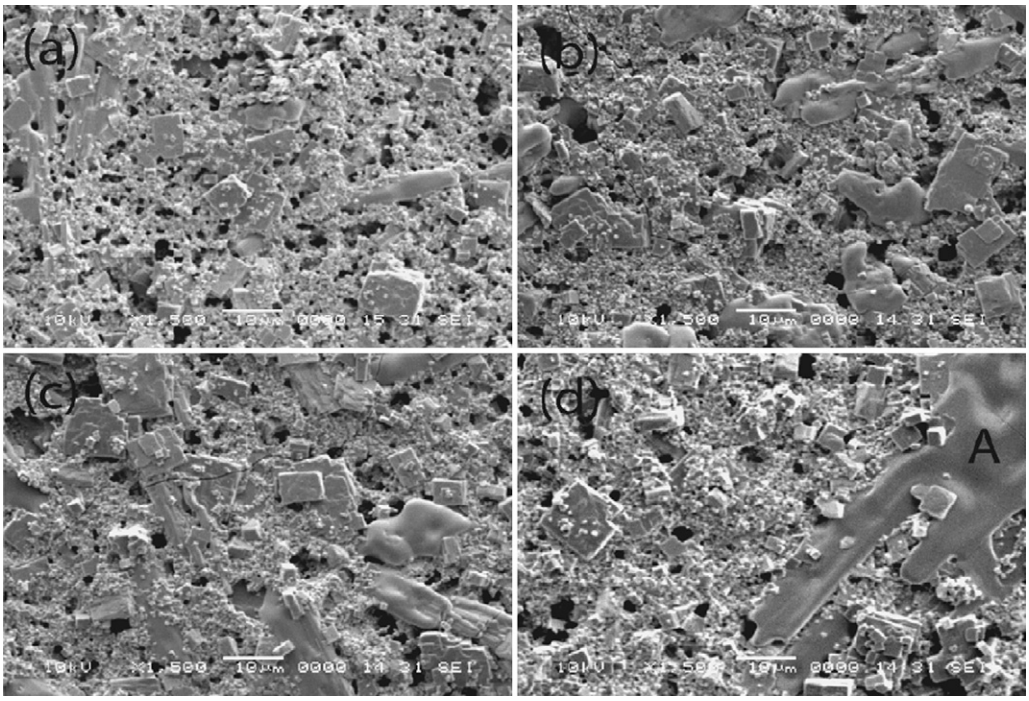

Fig. 2. SEM micrographs of KNN–xMn thick films (a) $x = 0$; (b) $x = 0.01$; (c) $x = 0.02$; (d) $x = 0.05$.

Fig. 4 shows the frequency dependences of the dielectric constant (ε) and loss tangent ($\tan\delta$) of the thick films. KNN thick films with Mn^{2+} doping displayed a large dielectric constant in contrast to undoped ones. The dielectric loss tangent of the films was reduced by Mn^{2+} doping at low frequency. The improvement in dielectric properties of KNN–xMn thick films should be attributed to the formation of the defect complex Mn_{Nb}–V_O [11]. This defect complex had a dipole moment and could be oriented to align the dipole along the direction of the applied electric field. Furthermore, the addition of Mn^{2+} compensated the charge defects which induced by the volatilization of alkali metal ions and enhanced the microstructure of the thick film. The reduction oxygen vacancies and the less porosity microstructure reduced the conduction loss consequently the dielectric loss at low frequency decreased.

Fig. 5 shows the J–E characteristics of the KNN–xMn thick films. Two distinctive regions are observed for KNN–xMn ($x = 0$, 0.01, 0.02 and 0.05) thick films. The leakage current density increases rapidly in the low voltage region and remains in a narrow band in the high voltage [12]. The leakage current density of the thick film with $x = 0.05$ stabilizes even at the voltage above 2 kV/cm. The leakage current density demonstrates significant improvement with the increase of Mn^{2+}. It reduced from the order of 10^{-4} to 10^{-8} A/cm^2 with adding 5% Mn ions. The low leakage current in the Mn^{2+} doped KNN thick films can be ascribed to the acceptor behavior of Mn ions and the compensation effect on the charge defects. The Mn ions formed the defect complex Mn_{Nb}–V_O and then decreased the free oxygen vacancy concentration. Furthermore, the charge defects residual by the volatilization of alkali metal ions is compensated by the addition of Mn^{2+} and consequently reduced the leakage current density.

Fig. 6 shows the unipolar electric field-induced strain curves of KNN–xMn ($x = 0$, 0.01, 0.02 and 0.05) thick films. The d^*_{33} defines as S_{max}/E_{max} and the values are illustrated in Fig. 6. The S_{max} and E_{max} presented the maximum strain and electric field,

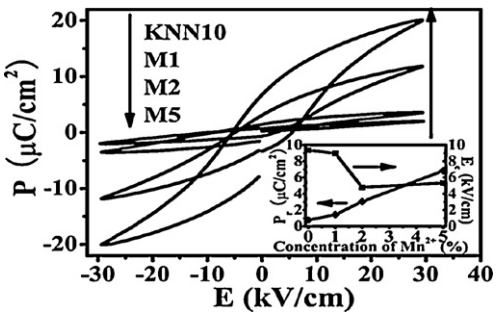

Fig. 3. Polarization hysteresis loops of KNN–xMn ($x = 0$, 0.01, 0.02 and 0.05) thick films at 30 kV/cm.

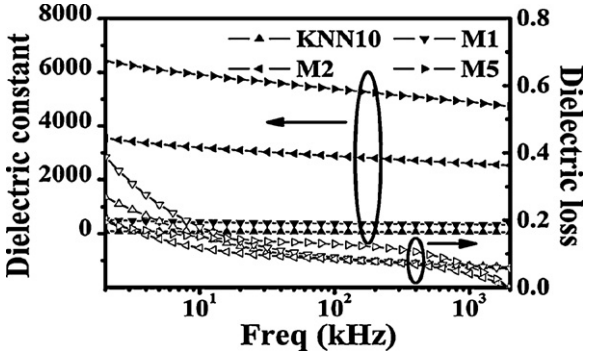

Fig. 4. Frequency dependency of the dielectric constant and loss tangent of KNN–xMn ($x = 0$, 0.01, 0.02 and 0.05) thick films.

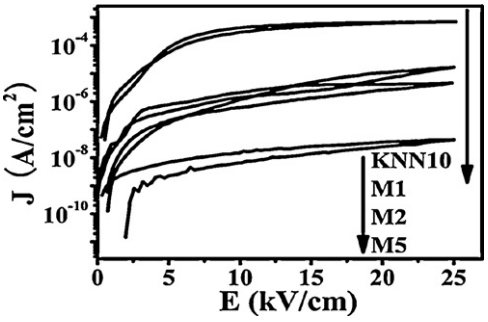

Fig. 5. *I–V* characteristics of KNN–*x*Mn ($x = 0$, 0.01, 0.02 and 0.05) thick films.

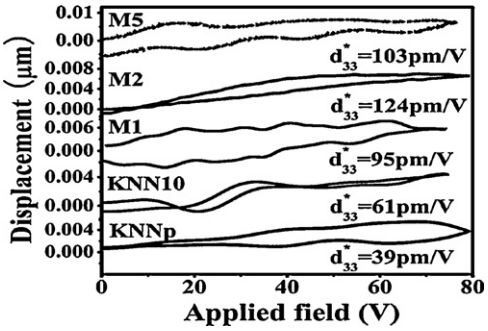

Fig. 6. Unipolar electric field-induced strain curves of KNN–*x*Mn ($x = 0$, 0.01, 0.02 and 0.05) thick films.

respectively. The d_{33}^* of textured KNN thick film (KNN10) showed 61 pm/V which is 60% higher than that of non-textured KNN (KNNp) thick film ($d_{33}^* = 38\,\mathrm{pm/V}$). The d_{33}^* increases with the addition of Mn^{2+} and reaches to the maximum value of 124 pm/V for the thick film with $x = 0.02$. The addition of Mn^{2+} reduces the charge defects and result in the decrease of the pinning centre which facilitated the domain switch. Furthermore, the decrease of the leakage current density weakens the internal electric field and thus increases the effective electric field. The d_{33}^* decreases to 103 pm/V by adding with 5% Mn^{2+}. The excessive Mn ions are supposed to act as an acceptor and became to be the new domain pinning centre which result in the reduction of d_{33}^* value.

4. Conclusions

The textured KNN thick films with Mn^{2+} doping were fabricated by using NN plate-like templates via the RTGG method. The films exhibit a perovskite structures. The Mn^{2+} dopants improve the microstructure of the thick film with $x = 0.02$. The F value of the thick film decreases a little with the addition of Mn^{2+}. The addition of Mn^{2+} effectively improves the ferroelectric polarization of the thick film. The P_r increases to 6.82 μC/cm² for the thick film with $x = 0.05$. The dielectric constant of the films is also improved and the dielectric loss is reduced at low frequency. A significant reduction in the leakage current density can be achieved by adding Mn^{2+} in the thick film. The piezoelectric constant d_{33}^* increases with the addition of Mn^{2+} and reaches to the maximum value of 124 pm/V for the thick film with $x = 0.02$.

Acknowledgements

The authors would like to acknowledge the support from the National Natural Science Foundation of China under grant Nos. 50972108, 50932007 and Shanghai Foundation Project under grant 08JC1419100. It was also partially supported by the Research Grants Council of the Hong Kong Special Administrative Region, China (CityU No. 103307).

References

[1] P. Muralt, M. Kohli, T. Maeder, A. Kolkin, K. Brooks, N. Setter, R. Luthier, Fabrication and characterization of PZT thin-film vibrators for micromotors, Sensors and Actuators A 48 (1995) 157–165.
[2] A. Dutschke, J. Meinhardt, D. Sporn, Analysis of the phase content and Zr:Ti fluctuation phenomena in PZT sol–gel films with a nominal composition near the morphotropic phase boundary, Journal of European Ceramic Society 24 (6) (2004) 1579–1583.
[3] R.N. Torah, S.P. Beeby, M.J. Tudor, N.M. White, Thick-film piezoceramics and devices, Journal of Electroceramics 19 (2007) 95–110.
[4] J. Rodel, W. Jo, K.T.P. Seifert, E.M. Anton, T. Granzow, D. Damjanovic, Perspective on the development of lead-free piezoceramics, Journal of the American Ceramic Society 92 (6) (2009) 1153–1177.
[5] F. Gao, R.Z. Hong, J.J. Liu, Y.H. Yao, C.S. Tian, Effect of different templates on microstructure of textured $Na_{0.5}Bi_{0.5}TiO_3$–$BaTiO_3$ ceramics with RTGG method, Journal of the European Ceramic Society 28 (10) (2008) 2063–2070.
[6] S. Wada, K. Takeda, T. Muraishi, H. Kakemoto, T. Tsurumi, T. Kimura, Preparation of [1 1 0] grain oriented barium titanate ceramics by templated grain growth method and their piezoelectric properties, Japanese Journal of Applied Physics 46 (10B) (2007) 7039–7043.
[7] F. Gao, X.C. Liu, C.S. Zhang, L.H. Cheng, C.S. Tian, Fabrication and electrical properties of textured $(Na,K)_{0.5}Bi_{0.5}TiO_3$ ceramics by reactive-templated grain growth, Ceramics International 34 (2008) 403–408.
[8] D. Lin, K.W. Kwok, H.L.W. Chan, Effects of MnO_2 on the microstructure and electrical properties of $0.94(K_{0.5}Na_{0.5})NbO_3$–$0.06Ba(Zr_{0.05}Ti_{0.95})O_3$ lead-free ceramics, Materials Chemistry and Physics 109 (2–3) (2008) 455–458.
[9] K. Matsumoto, Y. Hiruma, H. Nagata, T. Takenaka, Electric-field-induced strain in Mn-doped $KNbO_3$ ferroelectric ceramics, Ceramics International 34 (2008) 787–791.
[10] F.K. Lotgering, Topotactical reactions with ferrimagnetic oxides having hexagonal crystal structures—I, Journal of Inorganic and Nuclear Chemistry 9 (2) (1959) 113–123.
[11] X.H. Hao, J.W. Zhai, J. Zhou, X.W. Li, X.W. Song, S.L. An, Enhanced dielectric properties of lead barium zirconate thin films by manganese doping, Applied Surface Science 256 (16) (2010) 4902–4905.
[12] K.T. Kang, I.D. Kim, M.H. Lim, H.G. Kim, J.M. Hong, Annealing effect on dielectric and leakage current characteristics of Mn-doped $Ba_{0.6}Sr_{0.4}TiO_3$ thin films as gate insulators for low voltage ZnO thin film transistor, Thin Solid Films 516 (2008) 1218–1222.